Crystal structure of bis(tetraethylammonium) bis[4,5-disulfanyl-1,3-dithiol-2-onato(2−)]nickelate(II) and spectroscopic and electrical properties of related oxidized complexes‡

Shuging Q. Sun, Bin Zhang, Peiji J. Wu and Daoben B. Zhu*,†

Institute of Chemistry, Chinese Academy of Sciences, Beijing, 100080, P.R.China

Bis(4,5-disulfanyl-1,3-dithiol-2-onato)nickelate anion complexes $[Ni(C_3S_4O)_2]^{2-}$ were prepared. A single-crystal structure analysis has been performed for the bis(tetraethylammonium) salt **1**: orthorhombic, space group $I4(1)acd$, $Z = 8$, $a = b = 19.605(3)$, $c = 16.217(5)$ Å. Full-matrix least-squares refinement based on 744 independent reflections with $I > 2\sigma(I)$ yielded an R factor of 0.0651. The geometry around the nickel atom is greatly distorted from square planar, with a dihedral angle of 17.4° between the dithiolate ligand planes. Although it is essentially an insulator, with an electrical conductivity of 1.4×10^{-8} S cm^{-1} measured for a single crystal at room temperature, some partially and completely oxidized nickel complexes as well as iodine-doped single crystals exhibit increased conductivities of 10^{-3}–10^{-2} S cm^{-1}. Electronic, IR, ESR and X-ray photoelectron spectra of these complexes are discussed.

Many electrically conducting materials derived from bis-[4,5-disulfanyl-1,3-dithiole-2-thionate(2−)]metal complexes $[M(C_3S_5)_2]^{n-}$ (M = Ni, Pd or Pt) have been investigated.[1] Up to now, six of them[2] have been found to undergo a superconducting transition under pressure. In addition, [ettf][Ni-$(C_3S_5)_2$] [ettf = ethylenedithiotetrathiafulvalene, *i.e.* 2-(1,3-dithiol-2-ylidene)-4,5-ethylenedithio-1,3-dithiole] has been found to be a superconductor at ambient pressure.[3] It was thus interesting to extend such investigations to other similar polysulfur-ligand complexes. 4,5-Disulfanyl-1,3-dithiol-2-onate (C_3S_4O) has been synthesized[4] but fewer studies have been carried out on either the synthesis or the electrical properties of $[M(C_3S_4O)_2]$ complexes.[5] Recently the bistable electrical switching properties in electrodeposited thin films based on $[Ni(C_3S_4O)_2]^{x-}$ anion complexes were discovered in our laboratory.[6] This encouraged us to investigate further the changing of the intra- and inter-molecular interaction due to the replacement of S by O.

This paper reports the crystal structure of $[NEt_4]_2[Ni(C_3S_4O)_2]$ as well as the spectral and electrical properties of its analogues and oxidized complexes. As far as we know, this is the first report of the crystal structure of a $[M(C_3S_4O)_2]^{2-}$ complex.

Experimental

Preparation of the complexes

$[NEt_4]_2[Ni(C_3S_4O)_2]$ **1**, $[NMe_4]_2[Ni(C_3S_4O)_2]$ **2** and $[NEt_4]_2$-$[Cu(C_3S_4O)_2]$ **3**. To 4,5-bis(thiobenzoyl)-1,3-dithiol-2-one (500 mg, 1.28 mmol) in dry degassed methanol (20 cm³) under an argon atmosphere, was added an excess of sodium methoxide in dry degassed methanol [70 mg (3 mmol) sodium in 5 cm³ methanol] and the mixture was stirred under argon for 0.5 h to give a dark red solution. The compound NiCl₂·6H₂O (150 mg, 0.63 mmol) was added followed by tetraethylammonium bromide (270 mg, 1.28 mmol) dissolved in dry degassed methanol (10 cm³). The mixture was stirred for 30 min to precipitate brown microcrystals of $[NEt_4]_2[Ni(C_3S_4O)_2]$ **1**, which were filtered off, washed with anhydrous methanol then with anhydrous diethyl ether, and air dried (yield 61%). Recrystal-

lization of this complex from acetonitrile under argon afforded dark green crystals, which were used for structure analysis and electrical measurement. Similarly, brown microcrystals of $[NMe_4]_2[Ni(C_3S_4O)_2]$ **2** (68%) and $[NEt_4]_2[Cu(C_3S_4O)_2]$ **3** (64%) were obtained by using NMe₄Br or NEt₄Br and NiCl₂·6H₂O or CuCl₂·2H₂O.

Oxidized $[Ni(C_3S_4O)_2]^{x-}$ complexes. An acetonitrile–acetone (1:1) solution (15 cm³) of iodine (100 mg, 0.39 mmol) was added to complex **1** (100 mg, 0.15 mmol) dissolved in the same solvent (40 cm³). The mixture was stirred for 30 min to give a black precipitate of $[Ni(C_3S_4O)_2]$ **4** which was filtered off, washed with acetonitrile and diethyl ether, then dried in air (87% yield based on **1**).

Finely powdered complex **1** (100 mg, 0.15 mmol) was suspended in a solution of iodine (200 mg, 0.78 mmol) in diethyl ether (30 cm³). The suspension was stirred for 1 d at room temperature under an argon atmosphere. The resulting solid $[NEt_4]_2[Ni(C_3S_4O)_2]I_{7.8}$ **5** was filtered off and dried in air. The complex $[NEt_4]_2[Ni(C_3S_4O)_2]I_{2.3}$ **6** was obtained when **5** was washed extensively with diethyl ether. The salt $[NEt_4]_{0.17}$-$[Ni(C_3S_4O)_2]$ **7** was obtained by galvanostatic anode oxidation of **1** (10^{-3} mol dm^{-3}) in acetonitrile containing $[NBu^n_4][ClO_4]$ (5×10^{-2} mol dm^{-3}) as supporting electrolyte. A two-compartment cell where the anode and the cathode are separated by a medium-porosity frit was used with platinum electrodes (diameter 1 mm). The current was held constant at 1 μA. After 2 weeks the polycrystalline powders adhering to the anode electrode were collected, washed with acetone and dried in air.

Iodine-doped single crystals of complexes 1 and 2. These experiments were carried out using a capsuled bottle filled with iodine vapour. The typical size of the crystal was $1 \times 0.3 \times 0.2$ mm. Two gold-wire electrodes were glued to the crystal by gold-conducting paste.

Elemental analysis for the complexes obtained are listed in Table 1.

Physical measurements

Electronic absorption spectra were recorded on a Sigmazu UV-3100 spectrophotometer, electronic powder reflectance spectra

Table 1 Elemental analyses * for the complexes obtained

	Analysis (%)					
Complex	C	H	N	S	Ni	I
1 $[NEt_4]_2[Ni(C_3S_4O)_2]$	38.9	5.9	4.0	37.6		
	(38.9)	(5.9)	(4.1)	(37.7)		
2 $[NMe_4]_2[Ni(C_3S_4O)_2]$	29.7	4.2	5.0	45.0		
	(29.6)	(4.2)	(4.9)	(45.7)		
3 $[NEt_4]_2[Cu(C_3S_4O)_2]$	38.5	5.8	4.0			
	(38.6)	(5.85)	(4.1)			
4 $[Ni(C_3S_4O)_2]$	17.9	<0.3	0	61.0		
	(17.2)	(0)	(0)	(61.1)		
5 $[NEt_4]_2[Ni(C_3S_4O)_2]I_{7.8}$	15.7	2.5	1.5	15.9	3.6	58.8
	(15.8)	(2.4)	(1.7)	(15.3)	(3.5)	(59.3)
6 $[NEt_4]_2[Ni(C_3S_4O)_2]I_{2.3}$	27.1	4.3	2.6	27.2	6.1	29.9
	(27.2)	(4.1)	(2.9)	(26.4)	(6.05)	(30.1)
7 $[NEt_4]_{0.17}[Ni(C_3S_4O)_2]$	19.9	0.9	0.6	57.0	13.4	
	(20.0)	(0.8)	(0.5)	(58.1)	(13.3)	

* Calculated values in parentheses.

with a Sigmazu integrating sphere unit, IR spectra on a Bruker IFS-113 spectrophotometer using KBr pellets over the range 4000–400 cm^{-1}, ESR spectra on a Bruker ESP-300 spectrometer, X-ray photoelectron spectra on a Kratos ES-300 spectrophotometer and Raman spectra on a Nicolet FT-Raman 910 spectrometer. Cyclic voltammograms were measured in acetonitrile containing [NBu$_4$][ClO$_4$] as supporting electrolyte, using a conventional cell consisting of a glass–carbon and a platinum plate as working and counter electrode and a saturated calomel electrode (SCE) as reference. The resistivities of compacted pellets as well as single crystals were measured by using the conventional two-probe technique.[7]

Crystallography

Crystal data and data collection parameters for complex 1. $C_{22}H_{40}N_2NiO_2S_8$, $M = 679.75$, orthorhombic, space group $I4(1)/acd$ (no. 142), $a = b = 19.605(3)$, $c = 16.217(5)$ Å, $U = 6233(2)$ Å^3 (by least-squares refinement on diffractometer angles from 33 centred reflections, $10 < 2\theta < 24°$), $T = 293$ K, graphite-monochromated Mo-Kα radiation, $\lambda = 0.710\,73$ Å, $Z = 8$, $D_c = 1.449$ g cm^{-3}, $F(000) = 2864$, black plate with dimensions $0.8 \times 0.4 \times 0.1$ mm, transmission factors -0.304 to 0.432. Siemens P4 diffractometer, ω–2θ scan mode with left and right scan widths of 0.7, data collection range $2.08 < \theta < 25°$, h -1 to 23, l -1 to 23, k -1 to 19. Three standard reflections were monitored per 97 and showed no significant variation in intensity. 3288 Reflections measured, 1328 unique ($R_{int} = 0.0712$) and 774 $[I > 2\sigma(I_o)]$ were used in all calculations. Scattering factors were taken from ref. 8 and Lorentz-polarisation absorption was applied.

Structure solution and refinement. The structure was solved by the heavy-atom method, and subsequent Fourier-difference techniques, and refined anisotropically by full-matrix least squares on F^2 with SHELXL 93.[9] Hydrogen atoms were placed in calculated positions and not refined. The weighting scheme was $w = 1/[\sigma^2(F_o^2) + (0.0877P)^2]$, where the $P = (F_o^2 + 2F_c^2)/3$. The final $R = 0.0651$, $R' = 0.1498$, for 101 parameters and no restraint, goodness of fit = 1.215, maximum $\Delta/\sigma = 0.00$, $\Delta\rho = -0.023$ e Å^{-3}, without any chemical meaning.

During the structural refinement the carbon atoms bonded to N(1) and the terminal carbon atoms C(1), C(2) were disordered in two positions C(3), C(4) and C(5), C(6), having equal occupancy in the last refinement.

Atomic coordinates, thermal parameters, and bond lengths and angles have been deposited at the Cambridge Crystallographic Data Centre (CCDC). See Instructions for Authors, *J. Chem. Soc., Dalton Trans.*, 1997, Issue 1. Any request to the
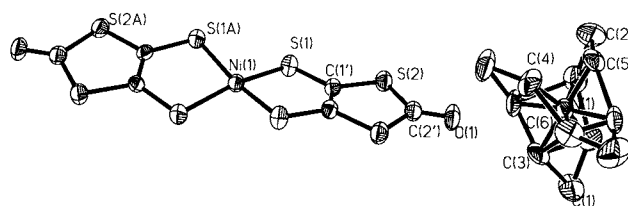

Fig. 1 Molecular geometry of $[NEt_4]_2[Ni(C_3S_4O)_2]$ **1** together with the atom-labelling scheme
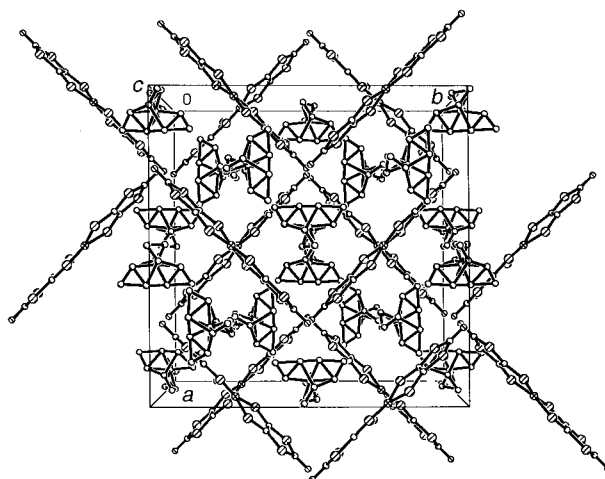

Fig. 2 Stereoscopic view of $[NEt_4]_2[Ni(C_3S_4O)_2]$ **1**

CCDC for this material should quote the full literature citation and the reference number 186/268.

Results and Discussion

Crystal structure of $[NEt_4]_2[Ni(C_3S_4O)_2]$ 1

The crystal structure of complex **1** consists of 16 NEt$_4$ moieties and 8 $[Ni(C_3S_4O)_2]$ anions in the unit cell. Fig. 1 shows the molecular geometry together with the atom labelling scheme and a stereoscopic view is given in Fig. 2. Selected bond distances and angles are summarized in Table 2. The atoms in the $[NEt_4]^+$ cation show considerable thermal motion and the standard deviations of the bond distances are therefore high. The nickel(II) ion is co-ordinated by four sulfur atoms. The nickel–sulfur distance [2.194(2) Å] is in better agreement with those in doubly negatively charged nickel dithiolene complexes,

Table 2 Selected bond distances (Å) and angles (°) with estimated standard deviations in parentheses for $[NEt_4]_2[Ni(C_3S_4O)_2]$ **1**

Ni(1)–S(1)	2.194(2)	S(1)–C(1′)	1.733(6)
S(2)–C(1′)	1.760(6)	S(2)–C(2′)	1.763(5)
O(1)–C(2′)	1.214(9)	C(1′)–C(1′B)	1.339(13)
S(1)–Ni(1)–S(1A)	93.22(9)	S(1)–Ni(1)–S(1B)	88.24(10)
S(1)–Ni(1)–S(1C)	167.04(10)	C(1′)–S(1)–Ni(1)	101.1(2)
C(1′)–S(2)–C(2′)	97.0(3)	C(1′A)–C(1′)–S(1)	122.3(2)
C(1′A)–C(1′)–S(2)	116.8(2)	S(2)–C(2′)–S(2A)	112.3(5)
S(1)–C(1′)–S(2)	120.9(4)	O(1)–C(2′)–S(2)	123.9(3)

Symmetry transformations: A $\frac{1}{2} + x$, $-y$, z, B $\frac{1}{4} - x$, $\frac{1}{4} - y$, $\frac{1}{4} - z$.
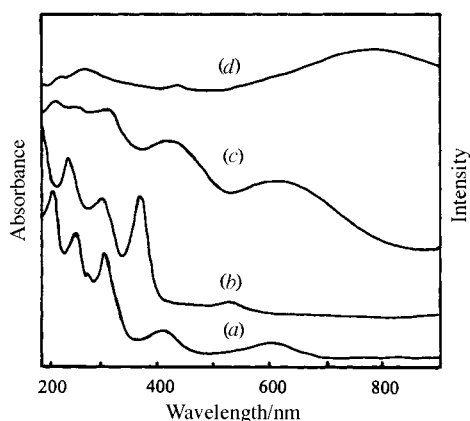

Fig. 4 The ESR spectra of $[NEt_4]_2[Cu(C_3S_4O)_2]$ **3** in the solid state (*a*) and in acetonitrile at room temperature (*b*), together with that of $[NEt_4][Ni(C_3S_4O)_2]$ in acetonitrile (*c*). G = 10^{-4} T

Fig. 3 Electronic absorption spectrum of complex **1** in acetonitrile (1.0×10^{-4} mol dm^{-3}) [newly resolved (*a*) and on standing for 1 d in air (*b*)] and powder reflectance spectra of **1** (*c*) and **4** (*d*)

i.e. 2.216(6) Å for $[\{Ni(C_3S_5)_2\}_2]$[10] and 2.166(6) Å for $[\{Ni(mnt)_2\}_2]$ (mnt = maleonitriledithiolate).[11] The carbon–sulfur distances 1.733(6), 1.760(6) and 1.763(5) Å have values intermediate between single (1.81) and double (1.71 Å) bonds, indicating a high degree of electron delocalization. Both of the carbon–carbon [1.339(13) Å] and carbon–oxygen [1.214(9) Å] distances are close to double-bond values (1.39 Å for C=C and 1.20 Å for C = O). The geometry around nickel is greatly distorted from planar, with a dihedral angle of 17.4° between the two C_3S_4O planes. This behaviour resembles that of $[NBu_4]$-$[Ni(C_3S_5)_2]$ and $[epy]_2[Cu(C_3S_5)_2]$ (epy = *N*-ethylpyridinium) for which the dihedral angles between the two ligand planes are 6.1 (ref. 12) and 57.3°.[13] Non-planarity around metal ions observed in C_3S_5 metal complexes, such as $[ttf][Pt(C_3S_5)_2]_3$,[14] is caused by a direct metal–metal interaction which induces the formation of $[\{Pt(C_3S_5)_2\}_2]$ dimers and thus folding of the normally planar $Pt(C_3S_5)_2$ unit (dihedral angle 11.2°). In the case of complex **1** there is no such evident theoretical reason for such a distortion. We can only assume that the distorted geometry may result from the packing effect of the anions or the negatively charged sulfur or oxygen of the ligand. No interaction between $[Ni(C_3S_4O)_2]^{2-}$ ions is observed, which results in the low conductivity of the complex.

Electronic and ESR spectra of the complexes

Fig. 3 shows the electronic absorption and powder reflectance spectra of complex **1**, together with the reflectance spectrum of neutral complex **4**. In spectrum (*a*) the absorption bands at 219, 262 and 310 nm are ascribed to local excitation of the C_3S_4O ligand and correspond to the bands at 224, 280 and 330 nm of $[NEt_4]_2[Zn(C_3S_4O)_2]$. Another $\pi \longrightarrow \pi^*$ transition is observed at 605 nm, which also corresponds to the band at 486 nm observed for $[NEt_4]_2[Zn(C_3S_4O)_2]$. The band at 410 nm observed in (*a*) is reasonably assigned to a Ni←S charge-transfer (c.t.) transition. These bands are similar to those of
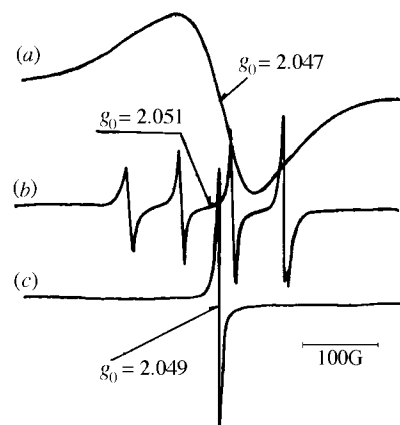
$[M(C_3S_5)_2]^{2-}$ complexes at around 224, 280, 310, 540 and 400 nm (due to local excitation of the C_3S_5 ligand and M←S charge-transfer transitions). The $\pi \longrightarrow \pi^*$ transitions of $[NEt_4]_2[Ni(C_3S_4O)_2]$ occur at shorter wavelengths than those of $[M(C_3S_5)_2]^{2-}$ anions. These differences obviously result from the different electron-withdrawing abilities of C=O and C=S. When the solution of complex **1** in acetonitrile was allowed to stand in air for some time all the bands were blue-shifted as illustrated in spectrum (*b*). That at 220 nm was shifted to lower wavelength and out of the spectrum; the bands at 262 and 310 nm were shifted to 248 and 306 nm with a slight decrease in intensity; and a Ni←S charge-transfer (c.t.) transition at 410 nm was also blue-shifted to 373 nm. Spectrum (*b*) is very similar to that of the $[Ni(C_3S_4O)_2]^-$ anions, indicating aerial oxidation from $[Ni(C_3S_4O)_2]^{2-}$ to $[Ni(C_3S_4O)_2]^-$ had occurred. It should be noted that although a strong absorption band at 384 nm owing to conjugation of the carbonyl group with the ethylene double bond[15] was observed for 4,5-bis(methylsulfanyl)-1,3-dithiol-2-one, the band at 373 nm for $[Ni(C_3S_4O)_2]^-$ could not be assigned to the same process. For $[M(C_3S_4O)_2]^{n-}$ ($n = 1$ or 2) the conjugation of the carbonyl group with the ethylene double bond was extended to the negatively charged sulfur atoms co-ordinated to the metal. This resulted in a red-shifted absorption band. The solid-state spectrum (*c*) of the present complex is essentially the same as the solution spectrum, indicating no significant electronic interaction among the complex ions in the solid state. In contrast, spectrum (*d*) exhibits a broad reflectance band around 760 nm, which may be due to an interaction among the neutral complex molecules.

Fig. 4 illustrates the ESR spectra of powder (*a*) and acetonitrile solution (*b*) of complex **3** as well as that of an acetonitrile solution of $[Ni(C_3S_4O)_2]^-$ (*c*). Complex **3** exhibits an isotropic spectrum ($g = 2.047$) in the solid state, which can be compared with the isotropic spectrum found for $[NMe_4]_2[Cu(C_3Se_5)_2]$ ($g = 2.074$) ($C_3Se_5 = 4,5$-diselanyl-1,3-diselenol-2-selenate).[16] A $^{63/65}$Cu hyperfine structure is observed ($g_0 = 2.051$, $A_0 = 67.4 \times 10^{-4}$ cm^{-1}) in the solution spectrum. The present A_0 value is rather close to that of $[epy]_2$-$[Cu(C_3S_5)_2]$[13] (66.5×10^{-4} cm^{-1}) and $[mb]_2[Cu(mnt)_2]$·Me_2CO[16] [mb = Methylene Blue cation; 3,7-bis-(dimethylamino)phenothiazin-5-ium] (68.4×10^{-4} cm^{-1}) containing non-planar $[Cu(C_3S_5)_2]^{2-}$ and $[Cu(mnt)_2]^{2-}$, respectively, and is much lower than $A_0 = 80.0 \times 10^{-4}$ cm^{-1} for the planar $[Cu(mnt)_2]^{2-}$ anion.[17] A drastic decrease in A_0 values in CuS_4 complexes was proposed to be caused by some distortion from a square-planar to a tetrahedral geometry around the copper atom.[18] Thus, the present $[Cu(C_3S_4O)_2]^{2-}$ complex seems to assume a geometry distorted from square planar in solution as $[Ni(C_3S_4O)_2]^{2-}$ in the solid state as discussed above. As shown in spectrum (*c*), there is a sharp band of

Table 3 Infrared $\tilde{\nu}(C{=}C)$ and $\tilde{\nu}(C{=}O)$ bands as well as binding energies of Ni $2p_{\frac{3}{2}}$ and S $2p_{\frac{3}{2}}$ electrons of the $[Ni(C_3S_4O)_2]$ complexes

			Binding energy/eV	
Complex	$\tilde{\nu}(C{=}C)/cm^{-1}$	$\tilde{\nu}(C{=}O)/cm^{-1}$	Ni $2p_{\frac{3}{2}}$	S $2p_{\frac{3}{2}}$
1	1474	1641s, 1601s	854.5	165.2, 163.6, 162.1
4	1273	1693vs, 1617w	855.3	165.3, 163.5, 162.2
5	1274	1695vs, 1617w	855.3	165.1, 163.7, 162.3

w = Weak, v = very, s = strong.

Table 4 Room-temperature electrical conductivities of the complexes

Complex	$\sigma/S\ cm^{-1}$	Complex	$\sigma/S\ cm^{-1}$
1	1.4×10^{-8} (s)	4	1.2×10^{-3} (p)
	1.6×10^{-3} (sd)	5	3.1×10^{-5} (p)
2	8.5×10^{-8} (s)	6	3.8×10^{-5} (p)
	9.2×10^{-4} (sd)	7	1.8×10^{-2} (p)
3	2.5×10^{-10} (s)		

s = Single crystal, d = after doping with iodine, p = compacted pellet.
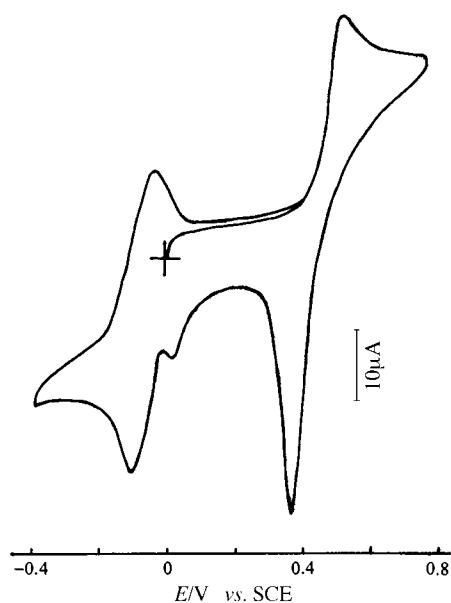
Fig. 5 Cyclic voltammogram of $[NEt_4]_2[Ni(C_3S_4O)_2]$ **1** (5×10^{-4} mol dm^{-3}) in acetonitrile containing $[NBu^n_4][ClO_4]$ (0.1 mol dm^{-3}), scan rate 100 mV s^{-1}

$[Ni(C_3S_4O)_2]^-$ in acetonitrile solution {obtained by aerial oxidation of $[Ni(C_3S_4O)_2]^{2-}$ in acetonitrile}, with an isotropic signal at $g_0 = 2.049$, which can be compared with that of $[NBu_4][Ni(C_3S_5)_2]$ ($g = 2.04$)[19] and $[NBu_4][Ni(C_3Se_5)_2]$ ($g = 2.095$).[16] However the ESR signals of the further oxidized species, complexes **4** and **5**, are very broad. This may be related to electron delocalization through the more effective conducting pathways of these complexes,[19] which leads to high conductivities.

Electrochemistry, IR and XPS study on complex 1 and its oxidized species

Fig. 5 illustrates the cyclic voltammogram of complex **1** in acetonitrile, which shows two sets of redox peaks. The first peak is centred at $E_1 = -80$ mV ($vs.$ SCE) and assigned to the one-electron reversible redox process between $[Ni(C_3S_4O)_2]^{2-}$ and $[Ni(C_3S_4O)_2]^-$. This E_1 value is less negative than that for the same redox process of $[Ni(C_3S_5)_2]^{2-}$ (-170 mV, $vs.$ SCE), due to the stronger electron-withdrawing ability of C=O than that of C=S. For the second redox couple the oxidation peak is not purely diffusion controlled but is also affected by modification of the electrode surface, for the backward peak is characteristic of a redissolution process, the intensity being proportional

to the scan rate.[20] This deposit probably comprises $[Ni(C_3S_4O)_2]^{-0.17}$ **7** which has been independently obtained by galvanostatic electrocrystallization. Therefore, the global scheme of the second oxidation step implies partial electron exchange according to $[Ni(C_3S_4O)_2]^- \longrightarrow [Ni(C_3S_4O)_2]^{x-} + (1 - x)e$, where $x = 0.17$. The small reduction peak at 20 mV ($vs.$ SCE) may also result from redissolution of the deposited material.

Finely powdered complex **1** suspended in diethyl ether reacted with an excess amount of iodine to give complex **5**. This has a Raman peak at 175 cm^{-1}, which may be assigned to the symmetric stretching of I_5^- or I_7^- ion.[21] When **5** was washed with diethyl ether extensively, **6** was obtained, and the Raman peak disappeared. X-Ray photoelectron spectroscopy (XPS) of this complex indicates only I$^-$ exists as described later. Similar to the metal–C$_3$S$_5$ complexes, the C=C stretching frequency of C$_3$S$_4$O–nickel complexes are very sensitive to the oxidation state. As shown in Table 3, the infrared band of complex **1** appears at 1474 cm^{-1}, whereas both **4** and **5** give a strong peak at $ca.$ 1274 cm^{-1}, with a very weak peak at the original frequency of **1** for **5** but not for **4**. The appearance of the band lowered by 200 cm^{-1} suggests the presence of two electron-oxidized C$_3$S$_4$O–nickel moieties, as evidenced by elemental analysis for complex **4**. The XPS studies also indicate that there is no nitrogen in **4**. In spite of the red-shift of the C=C stretching band, on the other hand, the C=O blue-shifted band is from 1641 and 1601 to about 1694 cm^{-1} upon complete oxidation. The valence state of the nickel atoms of the complexes can be deduced from the binding energies of the 2p electrons as determined by XPS. As shown in Table 3, complexes **4** and **5** exhibit larger binding energies than that of **1** suggesting noticeable oxidation of the metal, similar to that of C$_3$S$_5$–metal complexes.[22] In the case of **1** the ratio of the amounts of the two oxidation states of sulfur is nearly 1:1, however, in **4** and **5** the same two oxidation states are present, but the higher oxidation state is three times more populated than the lower. This indicates half of the sulfur co-ordinated to the metal is oxidized. It is interesting that the sulfur bound to the metal did not exist in the same oxidation state upon oxidation. Moreover, the I $3d_{\frac{5}{2}}$ binding energy of complex **6** is 619 eV, indicating the presence of I$^-$ in the complex.[23] The ratio of iodine and nickel estimated from relative intensities in the XPS spectra is about 2.1:1, consistent with the elemental analysis.

Electrical conductivities

The conductivity of the single crystal of complex **1** is somehow low, consistent with its crystal structure. However, the reflectance spectra of its oxidized complexes show broad bands at long wavelengths (see Fig. 3) which are not observed in the solution spectra. In accord with this the electrical conductivities of the oxidized complexes are significantly increased as described below.

When the single crystal of complex **1** was exposed to iodine vapour the conductivity increased from 10^{-8} to 10^{-4} S cm^{-1} within a few minutes; hours later the conductivity can be up to 10^{-3} S cm^{-1}. Prolonging the doping time resulted in reduction of the conductivity, the final value being around 10^{-4} S cm^{-1}, this may be due to complete oxidation of the complex. When

the conductivity had attained the maximum value, doping process was stopped, and the doped crystal 'dried' in vacuum (10^{-5} mmHg, *ca.* 1.33×10^{-3} Pa) for 1 d, the resistivity slightly increased from 40 to 48 kΩ, suggesting that a solid-state reaction occurred between I_2 and complex **1** during doping, rather than adsorption of I_2. The iodine doping of a single crystal of complex **2** leads to similar results. Table 4 summarizes the conductivity of the complexes, and it can be seen that the oxidized complexes exhibit higher conductivities. The highest conductor is the partially oxidized species. This is in accordance with the iodine doping of the single crystals. However, this process cannot be expected to occur inside the crystal, whereas the conductivity is estimated based on the total size; therefore, the conductivity of the compressed pellets is comparable with that of the doped crystal.

Acknowledgements

References

1 P. Cassoux, L. Valade, H. Kobayashi, A. Kobayashi, R. A. Clar and A. E. Underhill, *Coord. Chem. Rev.*, 1991, **110**, 115.
2 L. Brossard, M. Ribault, L. Valade and P. Cassoux, *Physica B (Amsterdam)*, 1986, **143**, 378; *Phys. Rev. B*, 1990, **42**, 3935; *J. Phys. (Paris)*, 1989, **50**, 1521; L. Brossard, H. Hurdequint, M. Ribault, L. Valade, J.-P. Legros and P. Cassoux, *Synth. Met.*, 1988, **27**, B157; A. Kobayashi, H. Kim, Y. Sasaki, R. Kato, H. Kobayashi, S. Moriyama, Y. Nishio, K. Kajita and W. Sasaki, *Chem. Lett.*, 1987, 1819; K. Kajita, Y. Nishio, S. Moriyama, R. Kato, H. Kobayashi, W. Sasaki, A. Kobayashi, H. Kim and Y. Sasaki, *Solid State Commun.*, 1988, **65**, 361; A. Kobayashi, R. Kato, A. Miyamoto, T. Naito, H. Kobayashi, R. A. Clark and A. E. Underhill, *Chem. Lett.*, 1991, 2163; H. Kobayashi, K. Bun, T. Naito, R. Kato and A. Kobayashi, *Chem. Lett.*, 1992, 1909.
3 H. Tajima, M. Inokuchi, A. Kobayashi, T. Ohta, R. Kato, H. Kobayashi and H. Kuroda, *Chem.Lett.*, 1993, 1235.
4 H. Poleschner, W. John, F. Hoppe and E. Fanghanel, *J. Prakt. Chem.*, 1983, **325**, 957.
5 I. Hawkins, R. A. Clark, C. E. Wainwright and A. E. Underhill, *Mol. Cryst. Liq. Cryst.*, 1990, **181**, 209; R. M. Olk, W. Dietzsch, K. Kohler, R. Kirmse, J. Reinhold, E. Hoyer, L. Golic and B. Olk, *Z. Anorg. Allg. Chem.*, 1988, **567**, 131; R. Vicente, J. Ribas, C. Faulmann, J.-P. Legros and P. Cassoux, *C. R. Acad. Sci.*, 1987, **305**, 1055; R. Vicente, J. Ribas, C. Zanchini, D. Gatteschi, J.-P. Legros, C. Faulmann and P. Cassoux, *Z. Naturforsch., Teil B*, 1988, **43**, 1137; S. G. Liu, P. J. Wu, Y. F. Li and D. B. Zhu, *Phosphorus Sulfur Silicon Relat. Elem.*, 1994, **90**, 219; S. G. Liu, Y. Q. Liu, S. H. Liu and D. B. Zhu, *Synth. Met.*, 1995, **71**, 137; J. X. Pan, Y. Q. Liu and D. B. Zhu, *Chin. Chem. Lett.*, 1995, **6**, 1077.
6 S. G. Liu, P. J. Wu, Y. Q. Liu and D. B. Zhu, *Mol. Cryst. Liq. Cryst.*, 1996, **275**, 211; S. G. Liu, Y. Q. Liu and D. B. Zhu, *Mol. Cryst. Liq. Cryst.*, 1996, **281**, 299.
7 S. Araki, H. Ishida and T. Tanaka, *Bull. Chem. Soc. Jpn.*, 1978, **51**, 407.
8 *International Tables*, Kluwer, Dordrecht, 1992, vol. C, Tables 4.2.6.8 and 6.1.1.4.
9 G. M. Sheldrick, SHELXL 93, University of Göttingen, 1993.
10 O. Lindqvist, L. Sjölin, J. Sieler, G. Steimecke and E. Hoyer, *Acta Chem. Scand., Ser. A*, 1979, **33**, 445.
11 R. Eisenberg and J. A. Ibers, *Inorg. Chem.*, 1965, **4**, 605.
12 O. Lindqvist, L. Anderson, J. Sieler. G. Steimecke and E. Hoyer, *Acta Chem. Scand., Ser. A*, 1982, **36**, 855.
13 G. Matsubayashi, K. Takahashi and T. Tanaka, *J. Chem. Soc., Dalton Trans.*, 1988, 967.
14 M. Bousseau, L. Valade, J.-P. Legros, P. Cassoux, M. Garbauskas and L. V. Interrante, *J. Am. Chem. Soc.*, 1986, **108**, 1908.
15 D. Y. Noh, M. Mizuno and J. H. Choy, *Synth. Met.*, 1993, **55–57**, 1705; *Inorg. Chim. Acta*, 1994, **216**, 147.
16 G. Matsubayashi and A. Yokozawa, *J. Chem. Soc., Dalton Trans.*, 1990, 3013.
17 D. Snaathorst, H. M. Doesburg, J. A. A. J. Perenboom and C. P. Keijizers, *Inorg. Chem.*, 1981, **20**, 2526.
18 U. Sakaguchi and A. W. Adisson, *J. Am. Chem. Soc.*, 1977, **99**, 5189.
19 Y. Sakamoto, G. Matsubayashi and T. Tanaka, *Inorg. Chim. Acta*, 1986, **113**, 137.
20 A. J. Bard and L. R. Faulkner, *Electrochemical Methods*, Wiley, New York, 1980.
21 M. A. Cowie, A. Gleizes, G. W. Grynkewich, D. W. Kalina, M. S. McClure, R. P. Scaringe, R. C. Teitelbaum, S. L. Ruby, J. A. Ibers, C. R. Kannewurf and T. J. Marks, *J. Am. Chem. Soc.*, 1979, **101**, 2921; R. C. Teitelbaum, S. L. Ruby and T. J. Marks, *J. Am. Chem. Soc.*, 1979, **101**, 7568; 1980, **102**, 332.
22 D. B. Zhu, M. X. Wang, P. Wang, D. H. Wang and S. H. Liu, *Kexue Tongbao*, 1986, **31**, 382.
23 T. Ohta, M. Yamada and H. Kuroda, *Bull. Chem. Soc. Jpn.*, 1974, **47**, 1158.